RSC Advances

ROYAL SOCIETY OF CHEMISTRY

www.rsc.org/advances

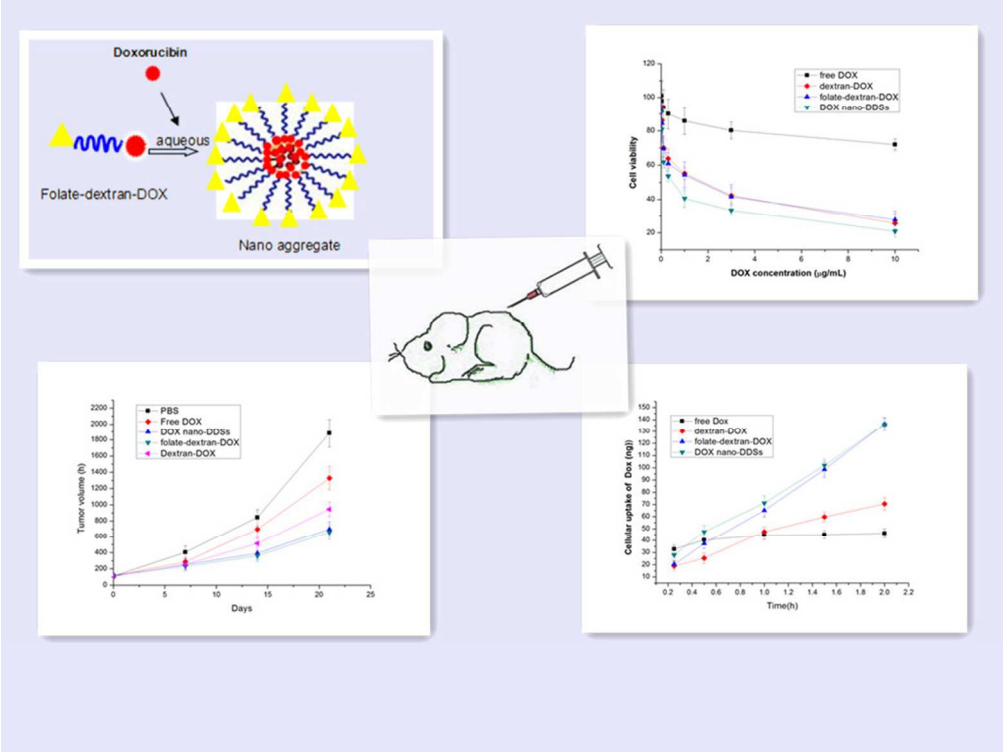

self-organized nano drug delivery systems (DOX nano-DDSs) with the function of both targeting tumor and controlling drug release was prepared, which exhibited larger drug release, higher cytotoxicity against HepG2/DOX cells, improved cellular uptake and decreased side toxicity. These results indicated that the DOX nano-DDSs have superior reversal efficacy to free DOX that serve as a highly promising nano-platform for future cancer therapy
361x270mm (72 x 72 DPI)

Self-organized nanoparticles drug delivery systems from folate-targeted dextran-doxorubicin conjugate loaded with doxorubicin against multidrug resistance

Yuannian Zhang[1+], Haili Wang[1+], Jean Felix Mukerabigwi[1], Min Liu[1], Shiying Luo[1], Shaojun Lei[1], Yu Cao[1,] *, Xueying Huang[1], Hongxuan He[2,] *

[1]Key Laboratory of Pesticide and Chemical Biology (Ministry of Education), College of Chemistry, Central China Normal University, Wuhan 430079, P. R. China.

[2]National Research Center for Wild life Born Diseases, Key Laboratory of Animal Ecology and Conservation Biology, Institute of Zoology, Chinese Academy of Sciences, Beijing 100101, China.

+: Equal contributors to the work

*: Author for correspondence

E-mail: caoyu@mail.ccnu.edu.cn

Tel: +86-27-61311087

Abstract: A folate-targeted dextran-doxorubicin conjugate (folate-dextran-DOX) for drug delivery systems (DDSs) was synthesized by grafting DOX onto the dextran through cleavable hydrazone bond, a pH-sensitive spacer for controlling drug release. Folate was coupled onto dextran as an ideal ligand for targeting hepatocytes. The conjugate was formulated into nanoparticles with excessive deprotonated DOX (DOX nano-DDSs) in aqueous condition, which exhibited larger size of 147.9 nm in diameter and improved drug entrapment at the level of 25.2%. *In vitro,* DOX nano-DDSs performed higher cytotoxicity and greater extent of intracellular uptake against drug resistant HepG2 (HepG2/DOX) cells. *In vivo* experiment displayed equivalent effect with folate-dextran-DOX micelles in terms of inhibiting tumor

volume and decreasing the toxicity, while it was significantly greater than free DOX. The result indicated that these targeted self-orgnized DOX nano-DDSs have superior reversal efficacy to free DOX that serve as a highly promising nano-platform for future cancer therapy.

Key words: Nanoparticle drug delivery systems (DDSs); Polymer drug conjugate; Folate-targeted; Hydrazone; Tumor.

1. Introduction

Polymer conjugate for anticancer drug delivery systems (DDSs) have been extensively developed due to their advantages. However, their drug efficacy was limited by the rapid clearance of the reticuloendothelial system (RES)[1-3]. Recently, the nanoscaled DDSs (nano-DDSs) utilizing polysaccharides as drug deliver exhibited dramatic decreasing impact of RES. Their hydrophobic core and hydrophilic shells assist them to form stable nanoparticle spontaneously, which present prolonged systemic circulation and sustained release of drug into the blood stream[2,4]. They are also appreciated for several natural characteristics such as biodegradability, water-solubility and non-antigenicity[5,6]. In addition, the enhanced permeable retention (EPR) effect resulting from the hypervasacular permeability and impaired lymphatic drainages allows the nano-DDSs to accumulate in tumor by "filtration" mechanism[7-10].

Currently, a pH-sensitive nano-DDS based on polymeric chains for delivery of drug have attracted interest[11-15]. Comparing with the traditional spacers that are less sensitive to the environment, hydrazone bond, in particular, are cleavable under mildly acidic conditions and stable under neutral pH conditions, which are facile to

control the drug release[16-19]. Therefore, the combination of drug and polymer through hydrazone bond contribute to the relative larger amount of drug release in tumor tissue by preventing from the cleaving in plasma.

Drugs of peripheral toxicity such as doxorubicin (DOX) performed a broad spectrum of antitumor behavior, which are easily extruded from the cell due to the emergence of multidrug resistant (MDR).[20] Their low drug efficiency as well as notorious side effect serves to diminish the therapeutic efficacy drastically. To overcome these obstacles, nano-DDSs should be manipulated with tumor-targeting ligands. One of the best candidates is folate acid, whose receptor has been known to be vastly overexpressed in several human tumor cells[21-28]. By conjugating folate, the micelles can be directed to cancer cells and subsequently internalized by folate-mediate endocytosis[4,22,24,29,30]. Therefore, the folate-targeted nano-DDSs could achieve both the decrease of the side effect by selectively locating in targeted cells and the increase of uptake in tumor cells.

A pH-sensitive nano-DDS based on pullulan for drug delivery systems was synthesized and *in vitro* cytotoxicity confirmed its improved drug release behavior in previous study[31]. In order to increase the cellular uptake and decrease the toxicity, however, we took further step to develop targeted nano-DDSs and implement more comprehensive tests through *in vivo* experiment. In our study, DOX were chemically conjugated to dextran by the hydrazone bonds. Folate acid was also grafted onto it. It is desirable to incorporate the advantages of hydrazone spacers, targeted ligand as well as the natural biodegradable polysaccharide carrier.[32] Larger drug content was achieved when combined with excessive DOX in aqueous condition. The cytotoxicity of nano-DDSs against HepG2/DOX cells and the therapeutic effect on tumor cells implanted in mice were also observed.

2. Materials and methods

2.1. Materials

Dextran (MW 100,000) was purchased from Huzhou Langshexi Biotech. Co. in Zhejiang Province, China. Doxorubicin (DOX), 3-(4,5-dimethylthiazol-2-yl)-2,5-diphenyltetrazolium bromide (MTT), Folic acid, N-hydroxysuccinimide (HOSu) and hydrazine hydrate were obtained from Aldrich Chemical Co. China. Organic solvents were used without further purification. All other chemicals were commercially available analytical grade reagents unless otherwise stated.

2.2. 4-Nitrophenyl Chloroformate Activation of Dextran

Dextran (2 g, 12.3 mmol unites) and 4-dimethylaminopyridine (DMAP) (0.15g, 1.2 mmol) were added in 20 ml of DMSO/pyridine solution (vol. ratio 1/1). Then 4-nitrophenyl chloroformate (2 g, 10 mmol) was dissolved at 0 °C. The reaction was carried out for 24 h at 0 °C. At the end of reaction, the mixture was precipitated in an anhydrous ethanol. A white precipitate was obtained and rinsed repeatedly for three times with the same solvent. Dextran 4-nitrophenyl carbonate was finally dried *in vacuo* and was identified by FTIR. The carbonate content was determined by UV analysis after activated dextran hydrolysis in NaOH. The degree of actvation of dextran was determined by the hydrolysis of activated dextran in NaOH solution. Activated dextran (100 mg) was dissolved into 10 ml of 0.1 N sodium hydroxide solution and the absorption of the carbonate residue was monitored by UV–visible spectroscopy at 402 nm for the p-nitroaniline group. The content of carbonate was determined using Beer's law. (DS= 34 % (mol %)).

2.3. Synthesis of Dextran-hydrazide

Dextran-COO(C_6H_4)NO_2 (4.68 g) was dissolved in 50 ml dry DMF and 15.7 mL (30 equiv.) 80% hydrazine hydrate was added at room temperature. The mixture was keep at room temperature for 48 h with gentle oscillation. After removing the majority of solvent by vacuum distillation, the mixture was precipitated in anhydrous ether. The obtained dextran-hydrazide was freeze-dried and identified by FTIR. The DS was determined by oxidation reduction titration. During the process of titration, the caprylic hydrazide could be oxidized to carboxylic acid while potassium bromate was reduced to potassium bromide. The end of the reaction could be indicated via methyl orange, in which the pink fade (http://www.med126.com/pharm/2009/20090109143304_72296.shtml). (DS= 28 % (mol %)).

2.4. Synthesis of Dextran-DOX

17.3g dextran hydrazide was dissolved in 50 ml of DMF and excessive DOX·HCl (1.74 g) was added. The mixture was stirred at room temperature for 24 h while being protected from the light. The product was dialyzed (MWCO 8000 Da, Spectra/Por membrane RC) against water and then freeze-dried to obtain the dextran-DOX conjugate. The percentages of DOX in conjugation were measured by a UV-spectrophotometer in DMSO at 480 nm. The content of DOX in conjugates was determined using the absorbance at 480 nm by UV－visible spectroscopy[33]. A calibration curve was made by detecting different concentration of DOX solution at 480 nm. The absorption of conjugate was measured at 480 nm and then the DOX

content of conjugate was found by comparison with the calibration curve of DOX. (DOX=7.1 % (wt))

2.5. Synthesis of folate-dextran

4.4 g folic acid was dissolved in 200 mL DMSO. 4.2 g HOSu and 2.2 g dicyclohexylcarbodiimide (DCC) were then added. The mixture was stirred at room temperature. After 6 h reaction under dark, the by-product dicyclohexylurea was removed by filtration. 17.3 g dextran hydrazide was then added. The reaction was performed for 24 h and 200 mL deionized water was added to the mixture. The formation was filtrated and lyophilized to obtain dextran hydrazide folate. The conjugation percentages of folic acid were calculated by determining the amount of folate conjugated in folate-dextran-DOX in DMSO at 365 nm, respectively, which was 2.3% (wt).

2.6. Conjugation of DOX to the folate-dextran

1.83 g dextran hydrazide folate was dissolved in 50 ml of DMF, and excessive amount of DOX (1.74 g) was added. The mixed solution was oscillated at room temperature for 24 h in dark. The formation was dialyzed (MWCO 8000 Da, Spectra/Por membrane RC) against water and then freeze-dried to obtain the folated dextran-DOX conjugate. The conjugation was identified by FTIR and its percentages of DOX were calculated by a UV-spectrophotometer in DMSO at 480 nm to determine the amount of DOX in the conjugate (DOX= 6.5% (wt)). The content of DOX in conjugates was determined using the absorbance at 480 nm by UV – visible spectroscopy[33]. A calibration curve was made by detecting different concentration of DOX solution at 480 nm. The absorption of conjugate was measured at 480 nm and

then the DOX content of conjugate was found by comparison with the calibration curve of DOX.

2.7. Preparation and characterization of nano DDSs

The conjugation (100 mg) was dissolved in 10 mL DMSO and dialyzed (MWCO 8000 Da) against excessive deionized water at 4 °C for 3-4 days while exchanging the water every 8 h. The dialysate was obtained and filtrated with 0.45 μm membrane and then was freeze-dried for 3 days to shape the nanoparticles.

In order to acquire nano-DDSs loaded with DOX, 15 mg DOX was dissolved in anhydrous DMSO (10 mL), which contained triethylamine. The molar ratio of triethylamine to DOX was 2:1. The conjugation (50 mg) was added into the solution, mixing overnight in dark and cold environment. At the end of the reaction, the solution was dialyzed against excessive deionized water at 4 °C for 3-4 days while exchanging the water at 8 h intervals. By directly scattering the organic phase into the aqueous phase, the conjugation aggregated into nanoparticles spontaneously. Extensive dialysis against deionized water was proceeded to remove the unencapsulated DOX and triethylamine. The obtained novel nano DDS was filtrated with 0.45 μm membrane, centrifuged, separated and lyophilized.

2.7.1 Particle size and zeta potential measurement

Nanoparticle size and its distribution were measured by dynamic light scattering (DLS; Zetasizer 3000, Malvern Instruments LTD, UK). Transmission electron microscopy (H-600, Hitachi ltd, Japan) was also conducted at the accelerating voltage of 200k eV to observe the nanoparticles.

2.7.2 Drug entrapment efficiency

The entrapment percentages of DOX were calculated by determining the amount of DOX in the Nana-DDS in DMSO at 480 nm using a UV-spectrophotometer.

The DOX entrapment efficiency was calculated as follow:

$$EE = \frac{A - B}{A} \times 100\%$$

Where A was the amount of DOX added in system, and B was the amount of DOX in supernatant.

2.8 *In vitro* release of DOX from the nano-DDS

The release study was conducted in serum, phosphate buffered saline (PBS, pH 7.4) and PBS at pH 5.0 (pH of endosomes or lysosomes) at 37 °C with moderate stirring. The DOX nano-DDSs, folate-dextran-DOX, dextran-DOX (1mg/mL) was transferred in 10 mL of PBS to a dialysis tube. At selected time intervals, the whole medium was removed and replaced with fresh PBS. The drug content was detected by UV at 480 nm.[33] A calibration curve was made by detecting different concentration of DOX solution (0.5, 1, 2, 4, 8, 16 μg/mL respectively) at 480 nm.

2.9 *In vitro* cytotoxicity assay

2.9.1 Cell culture

HepG2 cells (Yanyu Biotech Co., LTD, Shanghai) were cultured and preserved in RPMI-1640 medium, supplemented with 10% fetal bovine serum. The drug resistant HepG2 (HepG2/DOX) cell line was developed from HepG2 cells incubated with DOX in a stepwise increasing concentration (from 0.01 to 2 μg/mL) for several

months. The drug resistant cells were obtained by removing the dead cells. The drug resistance was maintained by culturing the cells at 1 μg/mL DOX.

2.9.2 Cytotoxicity assay *in vitro*

The 3-(4, 5-diemethylthiazol-2-yl)-2, 5-diphenyl-tetrazolium (MTT) assay (Sigma Co. USA) was implemented to evaluate the *in vitro* cytotoxicity of the 4 formulations (dextran-DOX, folate-dextran-DOX, DOX nano-DDSs and free DOX). HepG2/DOX cells were respectively incubated with the three formulations at a dose equivalent to free DOX. Statistic was determined by cell viability. The reversal of MDR was evaluated by the IC_{50} value. Control groups were treated with physiological saline. The cell viability was calculated as follow:

$$\text{Cell viability} = \frac{B}{A} \times 100\%$$

Where A is the absorbance of control group and B is the absorbance of treated group.

2.9.3 Cellular uptake of drug

HepG2/DOX cells were respectively pre-incubated with the 4 formulations (dextran-DOX, folate-dextran-DOX, DOX nano-DDSs and free DOX) for 2 h at a dose equivalent to free DOX (100 μg/mL), while LO2 normal hepatocyte cells were pre-incubated with the folate-dextran-DOX for 2 h at same dose. 1 mL cell suspension (10^7 HepG2/DOX cells) was mixed with 300 mL TM-2 buffer solution (10 mmol/L Tris-HCl, pH 7.4, 2mmol/L $MgCl_2$, 0.5mmol/L PMSF) in ice bath for 5 min. The mixture was added with 300 μL 1.0% Triton X-100 and cultured in ice bath for 5 min.

The mixture was filtrated by the membrane (0.22 μm) for 6 times. 1 mL cell suspension (10^7 HepG2/DOX cells) was added with DOX standard solution with different concentration. 1 mL cell suspension (10^7 HepG2/DOX cells) was mixed with 300 mL TM-2 buffer solution (10 mmol/L Tris-HCl, pH 7.4, 2mmol/L MgCl2, 0.5mmol/L PMSF) in ice bath for 5 min. The mixture was added with 300 μL 1.0% Triton X-100 and cultured in ice bath for 5 min. The mixture was filtrated by the membrane (0.22 μm) for 6 times. The formulations were analyzed by HPLC with a Shimadzu HPLC system composed of and a SPD-10Avp ultraviolet detector (Shimadzu Corporation, Japan) and two pumps (LC-10Avp and LC-10AS) in reverse phase mode at different points of time. Extend-C18 column (4.6×250 mm I.D., 5μm) was used and the mobile phase for the analysis was methanol-acetonitrile-phosphate buffer (pH 5.0, 0.2 M) (50: 20: 30, v/v/v) with the flow rate of 0.5 mL/min. The drug content was detected by UV at 480 nm[33]. A calibration curve was made by detecting different concentration of DOX solution (0.014, 0.028, 0.056, 0.112, 0.168, 0.224 μg/mL respectively) at 480 nm. The absorption of conjugate was measured and then the DOX content of conjugate was found by comparison with the calibration curve of DOX.

2.10 *In vivo* studies

All work performed on animals was in accordance with the "Guidelines for the Care and Use of Laboratory Animals" published by the National Institute of Health (NIH Publication No. 85-23, revised 1985). And this study was supported by the Ethics

Committee of Central China Normal University. Informed written consent was obtained from all subjects prior to the study.

2.10.1 *In vivo* pharmacokinetic study

Every specific pathogen-free grade male BALB/c nude mouse (provided by the Experimental animal center of Wuhan Institute of Biological Products) was inoculated with 0.2 mL HepG2/DOX cell suspension (5×10^6 cells/mL) at right axillary region. After being incubated for three weeks, solid tumor growth was noticeably increasing in nude mice.

144 tumor-bearing mice were randomly divided into 4 groups of 36 mice each group and respectively injected with the dextran-DOX, folate-dextran-DOX, DOX nano-DDSs and free DOX at a single dose (equivalent dose of DOX = 10 mg/kg). At different time interval, 0.5 mL blood sample was withdrawn by retro-orbital venous plexus puncture from tumor-bearing mice (from 4 groups of 6 mice each group). The livers, hearts, tumors, and kidneys of all the mice were immediately separated and washed with Na_2HPO_4 buffer, followed by homogenization with ethyl acetate solvent. The DOX was extracted after being incubated with acidic isopropanol for 12 h at 4 ºC. The mixture was centrifugated at 1200 rpm for 15 min. The DOX concentration in the supernatant solution was detected by HPLC quantitatively. Free drug or released drug was extracted and determined without incubation by HPLC as described previously[34].

2.10.2 *In vivo* cytotoxicity of nano DDS against drug resistant HepG2/DOX cells in mice

Specific pathogen–free grade male BALB/c naked mice (provided by the Experimental animal center of Wuhan Institute of Biological Products, 4 weeks old, 20-22 g) were inoculated subcutaneously with HepG2/DOX cells (1×10^7 cells/animal). After 3 weeks, solid tumor growth was noticeably established in most mice, dextran-DOX, folate-dextran-DOX, DOX nano-DDSs and free DOX (equivalent dose of DOX = 4 mg/kg) suspended in PBS were injected to tail veins of animals every week for four doses (days 0, 7, 14, and 21). A major axis and a minor axis of tumors were measured using the calipers. Tumor volume was then measured. The survival time and number of long-term survivors (LTS) until day 50 were monitored.

2.11. Statistical analysis

Data was described as means ± standard deviations (SD) of multireplicated determinations. Results were analyzed by one-way evaluated of variance (ANOVA) with the Student–Newman–Keuls multiple comparisons or *t*-test when comparing the differences between the means of two groups at the same time point. Diversities at $P < 0.05$ were considered statistically significant.

3. Results

3.1 Synthetic routes of folate-dextran-DOX conjugate.

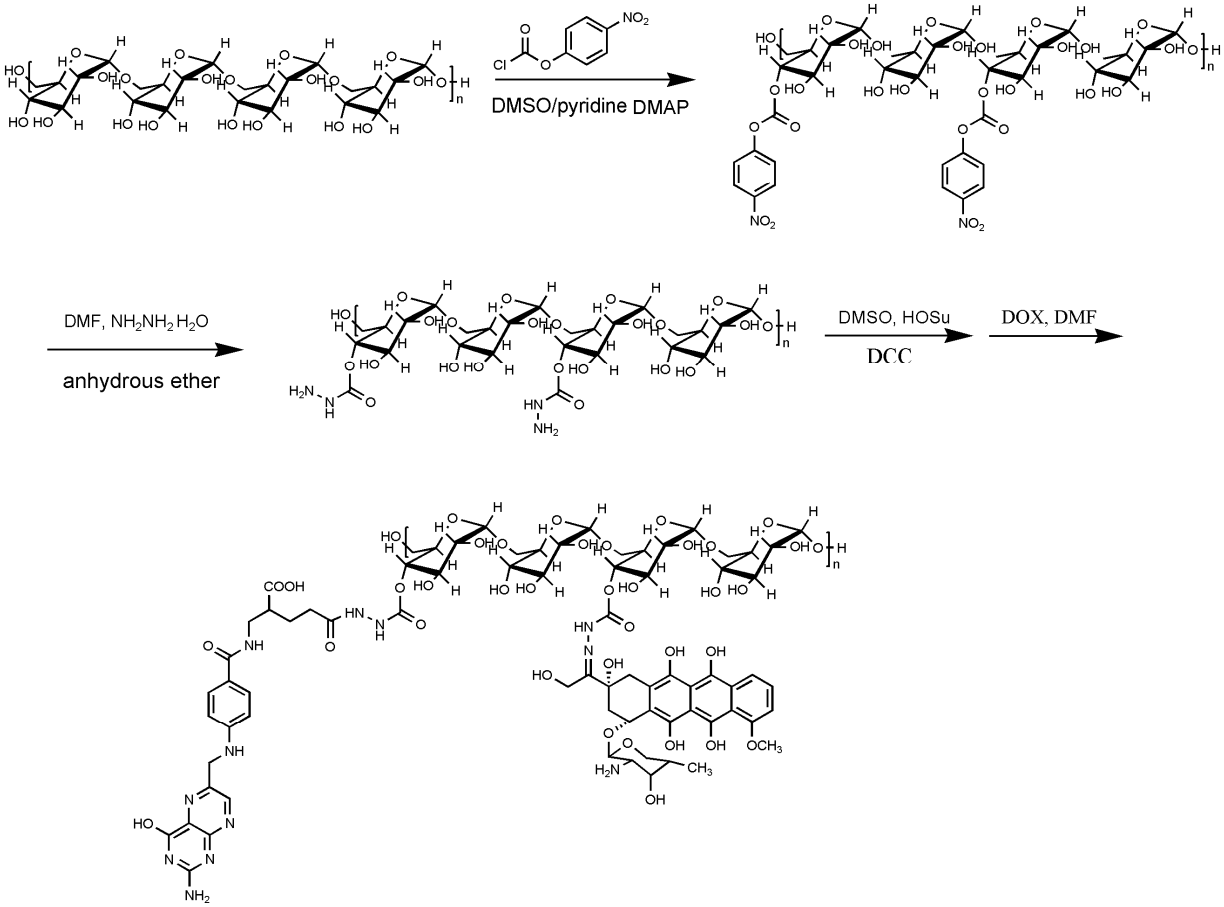

Fig 1. Synthetic route of folate-dextran-DOX conjugate

3.2 Preparation and Characterization of the Folate-Dextran-DOX Conjugate

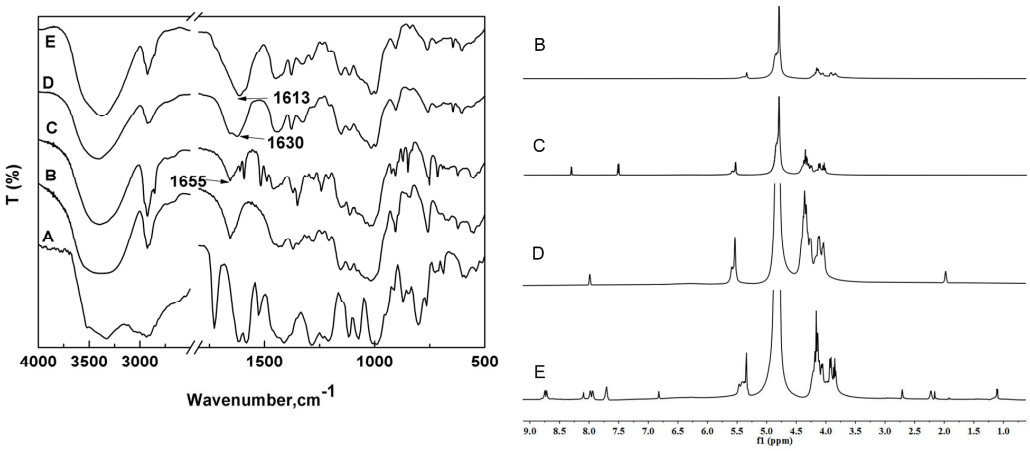

Fig. 2 FTIR (left) and ^{1}H-NMR (right) spectra of DOX (A), dextran (B), dextran hydrazide (D), 4-nitrophenyl-chloroformate-dextran (C) and folate-dextran-DOX conjugate (E).

The attachment of the DOX to the dextran was accomplished by hydrazone bond spacer, which was identified in Fig. 1. The peak around 1655 cm^{-1} might be the carboxylation of dextran, forming Dextran-COO(C_6H_4)NO_2. After amidation of the carboxylic group, the peak shifted to 1630 cm^{-1}, which indicated the embarking of the hydrazide to the activated dextran. The shifted peak about 1613 cm^{-1} might be attributed to the conjugating of DOX and folate. The content percentage of DOX, determined by the calculation and detection using UV-spectrophotometer, was approximately 6.5% (wt).

In the 1H NMR spectrum of Dextran-COO(C6H4)NO2, the new peaks at 8.31 ppm and 7.50 ppm compared with dextran was attributed to the protons on the benzene rings, which indicated the embarking of -COO(C6H4)NO2 groups. The signals at 7.98 ppm and 1.97 ppm were two kinds of protons in –NH-NH_2, besides, the signals of 8.31 ppm and 7.50 ppm were disappeared, which indicated the successful formation of dextran-hydrazide. In the spectrum of folate-dextran-DOX, the peak at 1.10 ppm was the result of methyl on DOX, which confirmed the conjugation of DOX. The peak at 8.72 ppm attributed to the proton on pyrazine was observed, indicating the conjugation of folate group.

A: δ 5.46 – 5.27 (m), 5.05 – 4.63 (m), 4.29 – 4.02 (m), 3.94 – 3.80 (m).

B: δ 8.31 (t, J = 5.6 Hz), 7.50 (d, J = 4.2 Hz), 5.74 – 5.46 (m), 4.81 (d, J = 17.6 Hz),

4.47 – 4.20 (m), 4.20 – 3.94 (m).

C: δ 7.98 (s), 7.98 (s), 5.55 (d, J = 20.8 Hz), 5.55 (d, J = 20.8 Hz), 4.79 (s), 4.29 (ddd, J = 26.8, 21.2, 14.4 Hz), 4.20 – 3.87 (m), 1.97 (s).

D: δ 8.72 (d, J = 10.2 Hz), 8.09 (s), 7.95 (d, J = 15.5 Hz), 7.70 (s), 6.81 (s), 5.52 – 5.30 (m), 5.19 – 4.50 (m), 4.25 – 4.03 (m), 3.90 (dd, J = 11.2, 8.6 Hz), 3.87 – 3.80 (m), 2.70 (s), 2.19 (d, J = 26.0 Hz), 1.10 (q, J = 3.5 Hz).

E: δ 8.72 (d, J = 10.2 Hz), 8.09 (s), 7.95 (d, J = 15.5 Hz), 7.70 (s), 6.81 (s), 5.52 – 5.30 (m), 5.19 – 4.50 (m), 4.25 – 4.03 (m), 3.90 (dd, J = 11.2, 8.6 Hz), 3.87 – 3.80 (m), 2.70 (s), 2.19 (d, J = 26.0 Hz), 1.10 (d, J = 5.1 Hz).

3.2. Characterization of DOX nano-DDSs

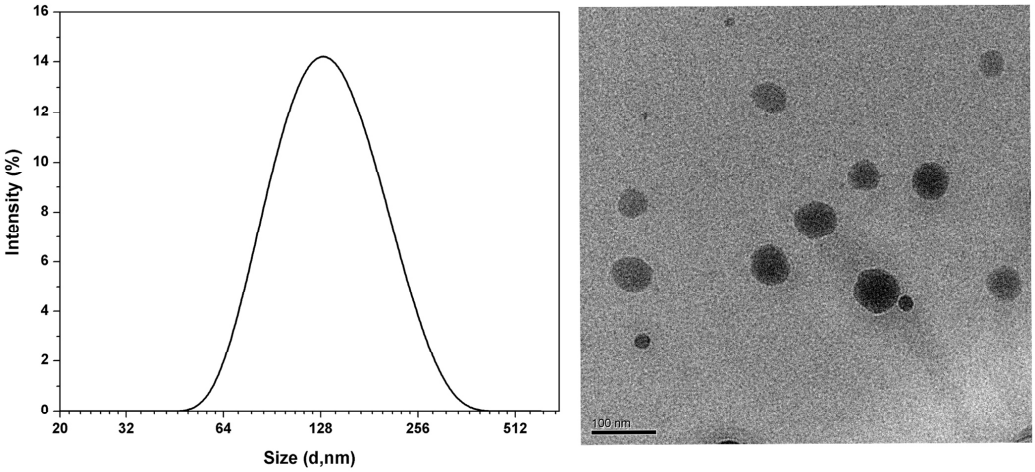

Fig. 3 Dynamic laser scattering (DLS) results (Left) and TEM micrograph (Right) of DOX nano-DDSs.

The morphology of these novel nano-DDSs loaded with DOX was shown in the transmission electronic microscope (Fig. 3). The mean diameter of the novel nano-aggregates is 147.9 nm with a PDI of 0.264, which was measured by DLS technique. The content of entrapped doxorubicin reached to 25.2% and was threefold higher than that of folate-dextran-DOX nanoparticles. The DOX entrapment efficiency was 81%.

3.3. DOX and folate released

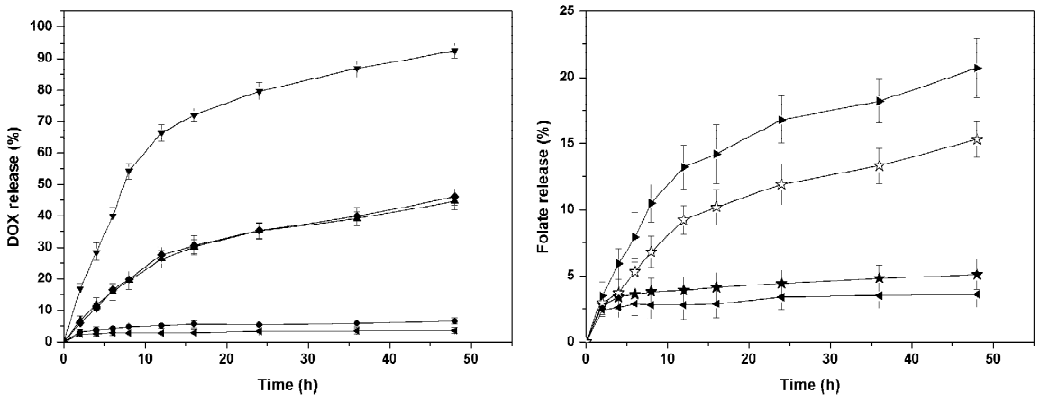

Fig. 4 Release profiles of DOX (left) and folate (right). (DOX release from DOX nano-DDSs（▼) (pH 5.0 buffer), DOX release from folate-dextran-DOX（▲) (pH 5.0 buffer), DOX release from dextran-DOX（◆), serum(●) and PBS(◀)(pH 7.4)), DOX release from DOX nano-DDSs (▶) (pH 6.5 buffer), folate release from folate-dextran-DOX（★) (pH 7.4 PBS), folate release from folate-dextran-DOX（☆) (pH 6.0 buffer)). Data were given as mean ± SD (n=6) (p<0.05).

The *in vitro* release behavior of four formulations was examined at different conditions. The result was shown in Fig. 4. In PBS at pH 7.4 and serum, the DOX released amount is negligible. While in buffer at pH 5.0, the drug release was

accumulated noticeably with time proceed. The release percentage of DOX nano-DDSs, folate-dextran-DOX and dextran-DOX after 48 h, was 92.5%, 44.7%, 46.1%, respectively. Compared with other administrations, the release from nano-DDSs loaded with DOX was faster and more thorough. There was no significant different release profile between folate-dextran-DOX and dextran-DOX conjugate. The amount of drug release of DOX nano-DDSs in pH 5.0 was drastically greater than that in pH 7.4, which indicated that the hydrazone bond is the appropriate spacer controlling drug release. The release percentages of folates was 15.3% in pH 6.0 buffer, which is 26.1% lower than that of DOX, indicating that folate was more stable than DOX when conjugated on the dextran in mild acidic environment therefore facilitated nano-DDSs to realize folate-mediated internalization in tumor cells.

3.4 *In vitro* cytotoxicity of the Nano-DDSs against Tumor Cells

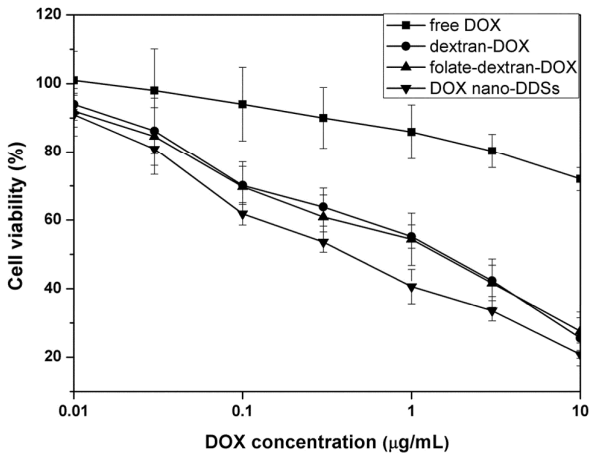

Fig. 5 *In vitro* cytotoxicity of free DOX(■), dextran-DOX(●), folate-dextran-DOX (▲) and DOX nano-DDSs(▼) against drug resistant HepG2/DOX cells. Data were given as mean ± SD (n=6) ($p<0.05$).

MTT-based *in vitro* cytotoxicity assay determined by the cell growth inhibition assay of the HepG2/DOX cells, was performed to compare therapeutic effect of DOX

nano-DDSs and other three formulations. According to the result shown in the Fig. 5, the DOX nano-DDSs nanoparticles showed better anti-cancer effect against tumor cells than that of free DOX. The calculated IC_{50} was 1.14 μg/mL, 1.09 μg/mL and 0.49 μg/mL for dextran-DOX, folate-dextran-DOX and DOX nano-DDSs, respectively, which indicated that nano-DDSs loaded with DOX performed better inhibition effect than that of folate-dextran-DOX and dextran-DOX.

3.5. Cellular uptake of DOX

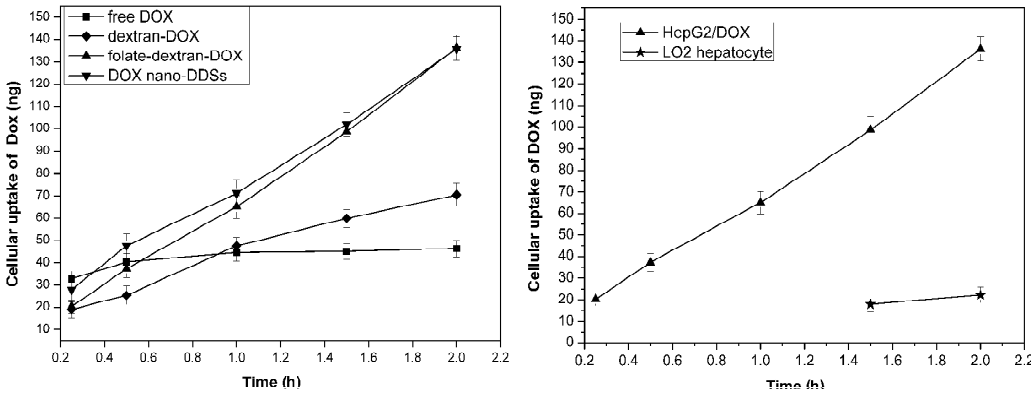

Fig. 6 Uptake of drug by MDR cells after incubated with free DOX (■), dextran-DOX（◆), folate-dextran-DOX (▲) and DOX nano-DDSs (▼) (Left) and uptake of DOX by folate-expressing cells versus LO2 hepatocyte cells (not express folate receptor)(Right). Values are means ± SD (n=3) (P<0.05).

HepG2/DOX cells were incubated in free DOX solution, dextran-DOX, folate-dextran-DOX and DOX nano-DDSs with equivalent dose of DOX for 2 h. The result was displayed in Fig. 6. DOX nano-DDSs and folate-dextran-DOX micelles both with the folate ligand, reached higher uptake amount of 135.9 ng and 135.2 ng, respectively after 2 h. In contrast, the dextran-DOX without targeting group showed

relatively lower uptake amount of 70.5 ng and free DOX was little internalized by tumor cells. The cellular uptake of DOX by LO2 normal hepatocyte at 2 hour was 22.3 ng, which was significantly lower than that by HepG2/DOX cells (136.2 ng), indicating that folate ligand on the prodrugs have selective targeting ability towards cells that express folate receptor.

3.6. *In vivo* pharmacokinetic study in tumor-bearing mice

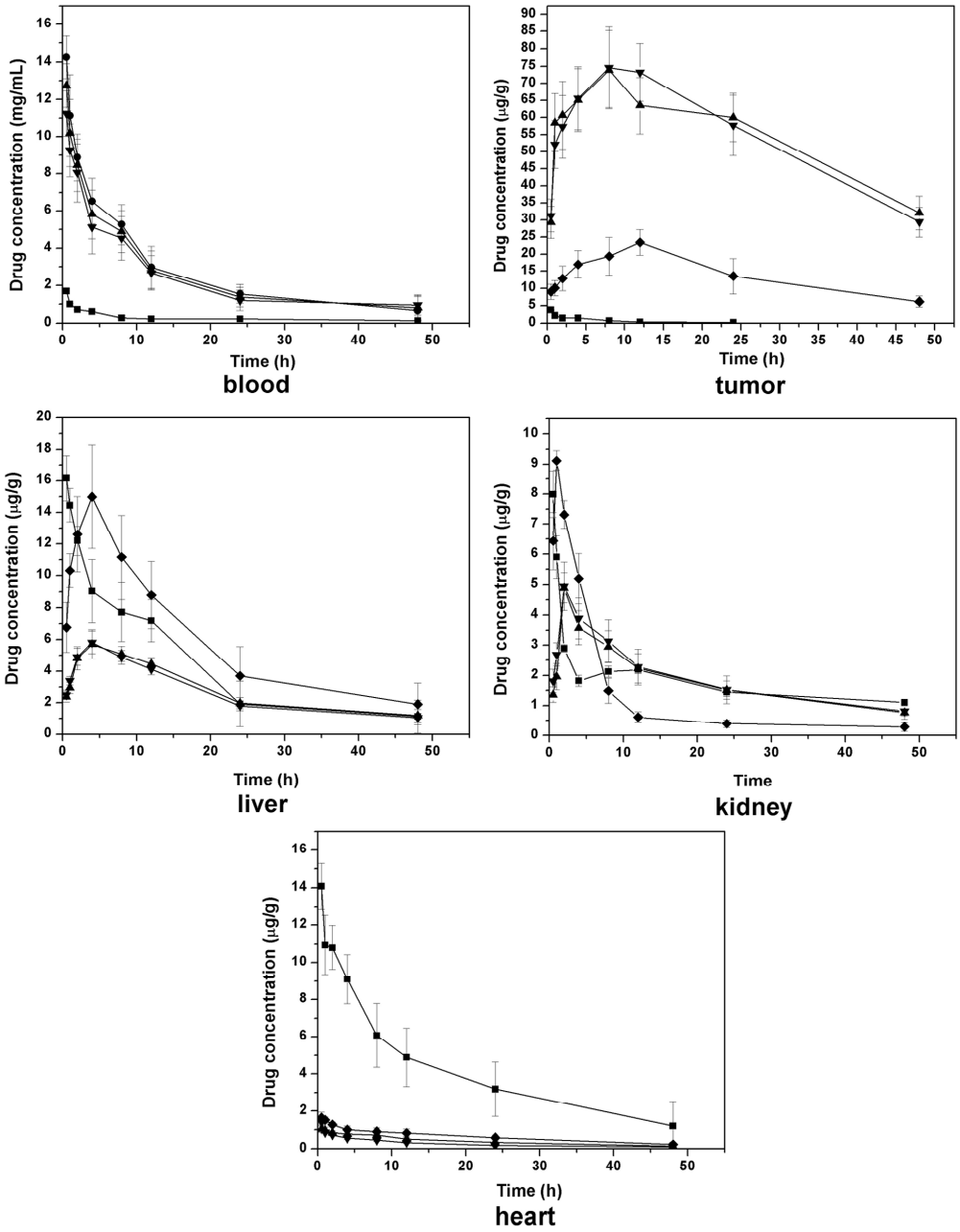

Fig. 7 Drug concentration-time profiles in different tissues after single dose of 10 mg/kg of free DOX (■), dextran-DOX（◆) folate-dextran-DOX (▲) and DOX nano-DDSs (▼) in tumor-bearing mice (n=12 per group). Values are means ± *SD* (n=3) (P<0.05).

Table. 1 Pharmacokinetic parameters of doxorubicin in tumor-bearing mice after i.v. administration of four formulations at a single dose of 10 mg/kg (P <0.05).

Tissue	Free DOX			Dextran-DOX			Folate-dextran-DOX			DOX-nano-DDSs		
	AUC	MRT	$T_{1/2}$	AUC	MRT	$T_{1/2}$	AUC	MRT	$T_{1/2}$	AUC	MRT	$T_{1/2}$
	μg/g*h	h	h	μg/g*h	h	h	μg/g*h	h	h	μg/g*h	h	h
Blood	5677	3.509	2.417	96130	7.234	5.001	90090	7.507	5.185	84170	7.834	5.411
Tumor	12.04	3.326	2.287	656.3	35.92	23.09	2552	67.82	46.41	2559	57.54	39.08
Liver	181.5	12.10	8.369	263.9	16.97	11.00	131.3	22.74	14.71	122.3	20.76	13.48
Kidney	21.17	2.33	1.597	45.41	4.355	2.655	78.33	19.39	12.68	81.08	18.56	12.21
Heart	159.9	12.73	8.805	28.18	21.05	14.57	18.88	21.06	14.58	8.698	7.370	5.092

Biodistribution profiles of DOX in blood together with other tissues were measured after administrating the four formulations DOX. The results are shown in the Fig. 7 and table.1.

In blood, the concentration of free DOX was 1.693 mg/L in 0.5 h, 7-fold lower than DOX nano-DDSs, which was attributed to the rapid elimination of the circulation system by passive convection. The DOX nano-DDSs and folate-Dextran-DOX performed nearly 20 times higher value of area under curve (AUC) than that of free DOX. Their mean residence time (MRT) reached to 7.834 μg/g*h and 7.507 μg/g*h, respectively, which was twofold greater than free DOX. These nano-DDSs showed excellent characteristic of prolonged circulation time before arriving at the tumor cell.

Significantly higher drug concentration, as we expected, was selectively distributed in tumor comparing with other RES organs including liver, heart and kidney. The AUC of DOX nano-DDSs in tumor was 21-fold higher than liver, 31-fold higher than kidney and nearly 300-fold higher than heart. The drug concentration of DOX nano-DDSs reached to maximum of 74.59 μg/g in 8 h and then decreased with relatively slower speed. The AUC values as well as MRT of DOX-nano-DDSs has no obvious difference with that of folate-dextran-DOX, while that was noticeably higher than that of free DOX and dextran-DOX.

In heart, negligible amount of DOX was detected in dextran-DOX, folate-dextran-DOX and DOX nano-DDSs as compared with the concentration of free DOX. The AUC of DOX nano-DDSs was 18 times lower than free DOX, indicating the reduced cardiac toxicity of DOX nano-DDSs.

3.7. Antitumor activity in *vivo*

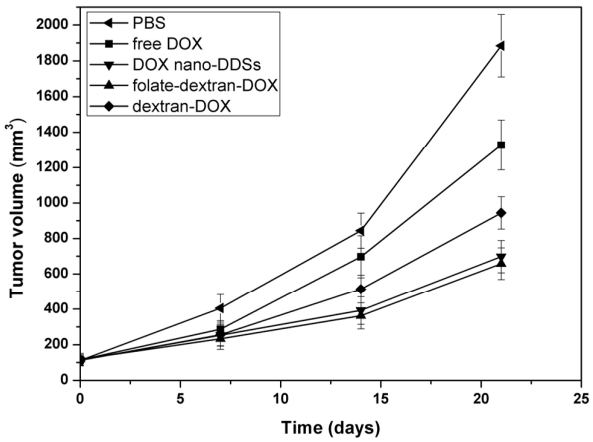

Fig. 8 Tumor volume changes in *vivo* of the xenograft nude mice bearing theHepG2/DOX tumors. (PBS (◀), free DOX (■), dextran-DOX (◆)

folate-dextran-DOX (▲) and DOX nano-DDSs (▼)). The tumor-bearing mice were treated with equivalent drug (4 mg/kg DOX) by tail injection every week for four dose (days 0,7,14, and 21).

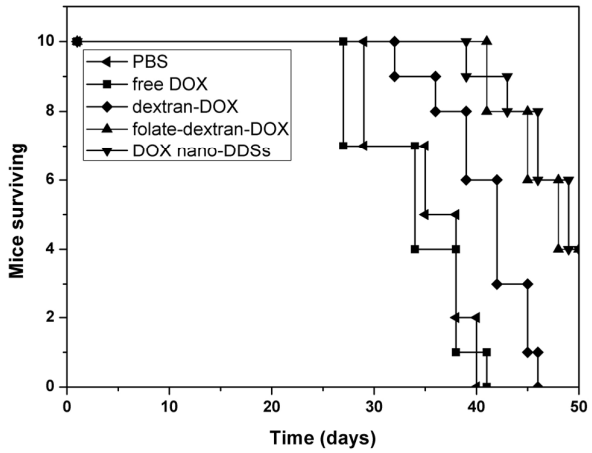

Fig. 9 Surviving profile of tumor-bearing mice treated with PBS (◀), free DOX (■), dextran-DOX（◆) folate-dextran-DOX（▲) and DOX nano-DDSs (▼) after injected HepG2/DOX cells. The tumor-bearing mice were treated with equivalent drug (4 mg/kg DOX) by tail injection every week for four dose (days 0,7,14, and 21). The survival time and number of long-term survivors (LTS) until 50th day were monitored ($p<0.05$).

In vivo cytotoxicity experiment of DOX nano-DDSs, folate-dextran-DOX dextran-DOX and free DOX against tumor cells was implemented in order to analyze the inhibition effect on growth of HepG2/DOX cells in mice. Consequently, nano-DDSs conjugated with folate ligand performed better therapeutic efficacy in suppressing the tumor cells as compared with that of non-targeted DOX. 20 days later, the volume of tumor treated with DOX nano-DDSs was about 47% less than that treated with free DOX. There is no significant different between two targeted nano-DDSs in terms of inhibiting the tumor volume (Fig. 8). In addition, targeted

nano-DDSs displayed longer life span of tumor-bearing mice than that of free DOX. As results, mice treated with DOX nano-DDS and folate-dextran-DOX showed longer life span (47.2 days and 46.8 days, respectively) compared with that of dextran-DOX and free DOX (40.8 days and 33.8 days, respectively) (Fig. 9).

4. Discussion

As a natural polysaccharide, dextran is an excellent polymeric carrier in drug delivery system due to the requisite properties of biodegradability, water-solubility and non-antigenicity. The amphipathic nano-DDSs (hydrophilic dextran and hydrophobic DOX) could stabilize in the aqueous environment, forming nano aggregates spontaneously. The decreased elimination impact by RES in circulation contribute noticeably to the prolonged circulation time, which could be explained statistically by higher MRT and AUC values of DOX nano-DDSs and folate-dextran-DOX over free DOX in blood (Table.1).

The content of DOX in the aggregates is 6.5%, which is probably restricted by the low drug loading efficiency and the instability of the high attachment. When combined with excessive free DOX, these self-assembled DOX nano-DDSs exhibited higher drug content, higher drug entrapment, greater size and higher entrapment efficiency (Fig. 3). The DOX nano-DDSs with the mean diameter of 147.9 nm (Fig. 3) could have access to the solid tumor tissue in a more facile way by EPR effect.

The drug releases of the DOX nano-DDSs are able to be controlled by the pH-sensitive spacer. The hydrazone bond could achieve highly hydrolysis in the acid condition of pH 5.0, a typical environment in tumor cell. This property can well be explained by the negligible drug release in the PBS at pH 7.4 and serum, comparing

with the prompt release in acidic condition (Fig. 4). *In vitro* cytotoxicity study demonstrated that HepG2/DOX cells bear higher chemosensitivity toward nano-DDSs than free DOX (Fig. 5), which could partly be explained by their higher drug release rate (Fig. 4). Although there is no significant difference between folate-dextran-DOX and DOX nano-DDSs in terms of cytotoxicity, after long treatment and because of the ample time to release drug, the DOX nano-DDSs with higher drug content, released drugs with faster speed and performed lower IC_{50} value (Fig. 5).

The DOX nano-DDSs not only have advantages in controlling drug release but also their targeted conjugate gave rise to enhanced drug uptake, decreased side effects and reversal of MDR. The efficacy of DOX was restricted by peripheral toxicity and in addition, its systemic injection has negligent effect on tumor regression and overall survival. Folate, an ideal targeting ligand, was covalently attached to the dextran carrier. The folate receptor on the tumor cell assists to internalize nano-DDSs by receptor-mediated endocytosis, which results in the significant effect in increasing intracellular uptake compared to micelles without folate ligand (Fig. 6). Based on the folate-receptor on the HepG2/DOX cells, nano-DDSs conjugated with folate could accomplish selective distribution in the tumor cells, locating sparsely on RES organs such as heart, kidney and liver (Fig. 7).

In vivo anti-cancer activities, targeted nano-DDSs showed superior effect in terms of delayed tumor volume growth, which was probably responsible for the synergetic impact of passive and active targeting. Passive targeting of nano-DDSs achieved the ‘filtration’ by EPR effect, while active targeting allows them to be internalized by

mediated receptor readily. On the other hand, the sustained release of DOX in nano-DDSs would contribute to the striking decrease in tumor size (Fig. 8).

5. Conclusion

The objective of this study was to develop self-organized nano-DDSs with the function of both controlling drug release and targeting tumor cells. The folate-dextran-DOX conjugate could form nanoparticles spontaneously in aqueous phrase. Larger mount of drug content could be achieved by adding free DOX into the micelles, reaching to 25.2%. Studies demonstrated the superior therapeutic effect of folate-dextran-DOX and DOX nano-DDSs as they exhibited excellent drug controlling, considerable drug release, improved cellular uptake and decreased side toxicity. Although the DOX nano-DDSs featured superior size and larger drug content, they performed negligible advantages over foalte-dextran-DOX, which allowed further study to be optimized.

Acknowledgment: This work was supported by the Scientific Research Foundation for the Returned Overseas Chinese Scholars (State Education Ministry, 2010-1174)

References

1. Min KH, Park K, Kim YS, Bae SM, Lee S, et al. 2008. *J Control Release,* **127**:208-218
2. Sutton D, Nasongkla N, Blanco E, Gao J. 2007. *Pharm Res,* **24**:1029-1046
3. Fatma J AS, Behling Cheng. 2013. *Chlin Physiol Funct Imaging,* **33**:293-301

4. Norased Nasongkla, Erik Bey, Jimin Ren HA, Chalermchai Khemtong, Jagadeesh Setti Guthi, et al. 2006. *Nano Letters,* **6**:2427-2430
5. Cao Y, Chen D, Zhao P, Liu L, Huang X, et al. 2011. *Ann Biomed Eng,* **39**:2456-2465
6. Chunli Zheng XL, Jiabi Zhu, Yuna Zhao. 2012. *Drug Development and Industrial Pharmacy,* **38**:653-658
7. D'Souza AJ, Topp EM. 2004. *J Pharm Sci,* **93**:1962-1979
8. Christie RJ, Grainger DW. 2003. *Adv Drug Deliv Rev,* **55**:421-437
9. Miyata K, Christie RJ, Kataoka K. 2011. *Reactive and Functional Polymers,* **71**:227-234
10. Nehoff H, Parayath NN, Domanovitch L, Taurin S, Greish K. 2014. *Int J Nanomedicine,* **9**:2539-2555
11. Song Y, Tian Q, Huang Z, Fan D, She Z, et al. 2014. *Int J Nanomedicine,* **9**:2307-2317
12. Qiu LY, Bae YH. 2006. *Pharm Res,* **23**:1-30
13. Pillay V, Seedat A, Choonara YE, du Toit LC, Kumar P, Ndesendo VMK. 2013. *AAPS PharmSciTech,* **14**:692-711
14. Marin E, Briceno MI, Caballero-George C. 2013. *Int J Nanomedicine,* **8**:3071-3090
15. Gregor Doerdelmann DK, Matthias Epple. 2014. *Journal of materials Chemistry B,* **2**:7123-7131
16. Melissa D. Howard AP, Allison Eckman, Michael Jay, Younsoo Bae. 2011. *Pharm Res,* **28**:2435-2446
17. Tao Jiang YML, Yin Lv, Yin Jia Cheng, Feng He, Ren Xi Zhuo. 2013. *Colloids and Surfaces B: Biointerfaces,* **111**:542-548
18. Guojun Mo XH, Shi Liu, Jun Yue, Rui Wang, Yubin Huang, Xiabin Jing. 2012. *European Journal of Pharmaceutical Science,* **46**:329-335
19. Hideaki Nakamura TE, PetrChytil, ManamiOhkubo, Jun Fang, Karel Ulbrich, Hiroshi Maeda. 2014. *Journal of Controlled Release,* **174**:81-87
20. Yu Cao YG, Lina Liu, Yi Yang, Peiguang Zhao, Ping Su, Liyan Liu Chao Qi,Xia Lei and Changjiang Yang.
21. Saul JM, Annapragada AV, Bellamkonda RV. 2006. *J Control Release,* **114**:277-287
22. Yoo HS, Park TG. 2004. *J Control Release,* **96**:273-283
23. Saul JM, Annapragada A, Natarajan JV, Bellamkonda RV. 2003. *Journal of Controlled Release,* **92**:49-67
24. Zhao H, Yung LY. 2008. *Int J Pharm,* **349**:256-268
25. Gabizon A, Shmeeda H, Horowitz AT, Zalipsky S. 2004. *Adv Drug Deliv Rev,* **56**:1177-1192
26. Varshosaz J, Hassanzadeh F, Aliabadi HS, Banitalebi M, Rostami M, Nayebsadrian M. 2014. *Colloid and Polymer Science,* **292**:2647-2662
27. Alireza Mehdizadeh SP, Ali Shakeri-Zadeh, Seyed Kamran Kamrava, Mojtaba Habib-Agahi, Mohammad Farhadi, Morteza Pishghadam, Amirhossein Ahmadi, Sanam Arami, Yuri Fedutik. 2014. *Lasers Med Sci* **29**:939-948
28. Emilia Moradi DV, Martin Garnett, Franco Falcone, Snow Stolnik. 2012. *RSC Advances,* **2**:3025-3033
29. Prabaharan M, Grailer JJ, Pilla S, Steeber DA, Gong S. 2009. *Biomaterials,* **30**:5757-5766
30. Xu Hua Liang YS, Lu Sha Liu, Ying Yong Zhao, Xiao Yun Hu, Jun Fan. 2012. *Chinese Chemical Letters,* **23**:1133-1136
31. Lu D, Wen X, Liang J, Gu Z, Zhang X, Fan Y. 2009. *J Biomed Mater Res B Appl Biomater,*

89:177-183

32. Li H, Bian S, Huang Y, Liang J, Fan Y, Zhang X. 2014. *Journal of Biomedical Materials Research Part A,* **102**:150-159
33. Yoo HS, Park TG. 2004. *Journal of Controlled Release,* **100**:247-256
34. Seymour LW, Ulbrich K, Strohalm J, Kopeček J, Duncan R. 1990. *Biochemical Pharmacology,* **39**:1125-1131